A Novel Methodology to evaluate Uplink Exposure by Personal Devices in Wireless Networks

Anis Krayni, Abdelhamid Hadjem, Alain Sibille, Christophe Roblin, and Joe Wiart, *Senior Member, IEEE*

***Abstract*—Over the last twenty years, the wireless technology has known a large development in terms of devices and services, accompanied consequently by considerable doubts about the level of exposure to the electromagnetic fields radiated by these systems. An intermediate step in the assessment of the real exposure is to statistically model the input power delivered to these personal devices during an uplink transmission. In this spirit, we propose a systematic methodology for the characterization of the variability of the delivered input power for given propagation conditions. This methodology first addresses the influence of the personal devices relative positioning, with respect to the users body on the antennas performance as well as on the exposure level. Secondly it addresses the sensitivity of the input power to the characteristics of the propagation channel. The exposure levels have been investigated from Specific Absorption Rates (SAR) computed using finite-difference time-domain (FDTD) simulations on a realistic numerical model of child bodys. The input power is directly related to the antenna radiation pattern and to the local propagation scenario, through effects such as body obstruction and multipath diversity. The statistical analysis shows that the delivered input power can be modeled by an inverse Gaussian or a Log-normal distribution.**

***Index Terms*—Human-body effect; EMF exposure; wireless devices; antenna theory; radio propagation; statistical analysis.**

I. Introduction

As a result of today's rapidly growing mobile telecommunications market, mobile network operators are asked to optimize their networks in order to ensure an efficient use of energy resources while maintaining compliance with recommended exposure limits [1]. This fact requires a deep knowledge of the propagation environment as well as a rigorous analysis of interactions between antennas on wireless devices and the human body [2-3].

Although the propagation environment has been the subject of a lot of research [4-5], the study of the interactions human body-antenna remains a complicated subject, due to the high variability of these parameters, such as the type of antenna and the body shape. These interactions have been often investigated toward two disjoint objectives. One is dedicated to analyze the effect of the antenna radiation on the human body whereas the second is devoted to study the effects of human body on the antenna performance. In wireless communications, the devices are usually placed close to the human body. Accordingly, a part of energy is necessarily absorbed. The whole body SAR (W/kg) expresses the average of the exposure over the whole body. It depends on many parameters, such as the design of the antenna and its position with respect to the human body [6].

Conversely, the antenna performance is significantly affected by close proximity to the human body. In short, a strong coupling effect takes place between the human body and the antenna [7], which generally severely affects its impedance and radiation pattern [8].

A rigorous evaluation of the true exposure requires a precise knowledge of the input power delivered to the personal devices. Usually, this uplink power depends on many factors, including the propagation channel, the antenna performance and the body shadowing effect (BSE) [9], for reasons recalled below.

Many efforts have been carried out in order to assess the uplink exposure, but they are based on experimental and numerical approaches with simplified human models [10-11] without either taking into consideration the impact of realistic postures or using a rigorous quantification of the power absorbed by the whole human body [12-14]. In addition, most or all of these studies just didn't take into consideration the impact of the propagation channel.

The contributions of the present study are as follows. Primarily, it aims to quantify the SAR using FDTD simulations [15]. Secondly, it focuses on implementing a systematic approach to characterize the variability of the input power delivered to a personal device, by combining its antenna gain with a suitably "realistic" propagation channel model [16]. To do so, two sets of numerical experiments have been carried out, which are part of a larger study within the framework of the European FP7 project LEXNET [17]. In the first, the user's body and his personal device in transmission mode are supposed invariant. During this investigation, the focus is mainly oriented towards both of the quantification of the SAR and the statistical characterization of the variability of the delivered input power, which stems from the user's random orientation with respect to a far line of sight (LOS) receiver.

In the second, we have analyzed the influence of the positioning of the personal device against the human body on the SAR and we have studied the variability of the delivered input power in both LOS and NLOS (Non-line of Sight) scenarios. The paper is organized as follows. Section II introduces the methodology intended to assess the variability of the delivered input power in the case of LOS scenarios, while taking into account the shadowing effects caused by human body. Section III describes the numerical tools used in this work to obtain realistic quantitative data. In section IV, we present the results obtained from exposure simulations and from the statistical analysis of the delivered input power. In section V, the influence of the device positioning on the exposure variability and on the degradation of the antenna gain is analyzed. In this part, we also analyze the distribution of the delivered input power, according to the position of the personal device and to the user orientation (with respect to the receiver antenna) in a LOS scenario. Finally, section VI contains a study of the influence of multipath propagation on the distribution of the delivered input power for a fixed position of the personal device, and is followed by a concluding section.

II. Methodology and approach

Throughout this section, we discuss the methodology and the assumptions used to characterize the variability of the input power delivered to a personal device during an uplink wireless communication. We denote as the transmitter system, the system formed by the personal device and the user body, and we consider the receiver system to be equipped with a fixed antenna (e.g., a base station). In a first step, we assume that the wireless communication is performed along a single dominant path, representing the *LOS*, characterized by a direction of departure (DoD) $(\phi_{LOS}, \theta_{LOS})$. In our analysis, the average distance between the transmitter system and the receiver antenna is assumed to be fixed without any impact on the conclusions. Hence, for a given frequency, the propagation path loss is constant [18].

During the communication, the input power delivered to the transmitter system depends fundamentally on the gain in the *LOS* direction. Since an antenna radiation pattern is usually anisotropic, this parameter varies after each change in the transmitter orientation with respect to the base station. An important aspect of the present work is to take into account realistically how the system takes a decision on the transmitted power. Indeed, for interference limitation reasons, the transmitted power is commonly adjusted to a minimum level, consistent with a predetermined link quality. Then, the delivered input power P_{in} must be simultaneously changed with the gain $G_e(\phi_{LOS}, \theta_{LOS})$ in order to meet the requirements of receiver in terms of signal to noise ratio (SNR)[19].

In practice, assuming a constant noise power, the received power (at the base station) must be such that, the same SNR is maintained in order to ensure a successful decoding. This means that the product of the input power delivered to the transmitting antenna (P_{in}) and of its power gain (G_e) in the *LOS* direction should be constant [21]:

$$P_{in} G_e(\phi_{LOS}, \theta_{LOS}) = \alpha \qquad (1)$$

It should be mentioned that G_e is the effective gain of the couple "user-antenna", which is the antenna gain calculated in the presence of the user's body. This takes into account the user-induced loss. On the other hand, P_{in} represents the total input power, which is equal to the sum of the power absorbed by the user's body and the useful power, which can be used to achieve the radio communication. In fact, we assume that the antenna is matched and lossless.

Firstly, the personal device is assumed to be placed in a fixed position with respect to the user's body. Thus, the user's body and the personal device compose an invariant transmitter system S. The sphere surrounding the system S represents the sphere on which the various parts of a radiation pattern are calculated. It is assumed to be fixed with respect to the base station, while the system S can rotate over azimuth and elevation angles. The orientation of the system S with respect to the base station axes is given by a random variable $\Omega_S(\phi_S, \theta_S)$, where ϕ_S and θ_S are respectively the angles of rotation of S around the vertical axis the vertical axis *z'Oz* and around the horizontal plane *xOy* (Fig.1).

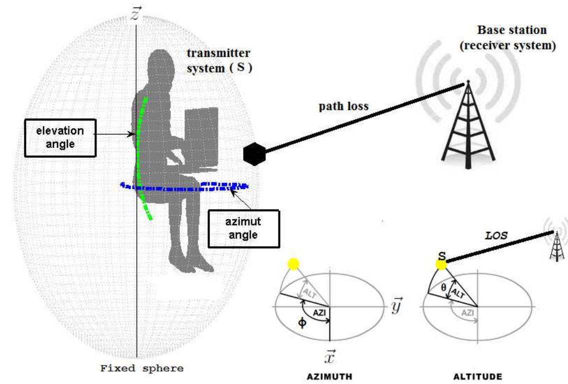

Fig. 1. Design concept.

Taking into account these design considerations, the original problem is restricted to the estimation of the delivered input power (P_{in}) for any realistic orientation of the system S that verifies the power constraint (1).

III. Numerical tools and FDTD simulations.

A. Human models

A 3D numerical whole body voxel model, *Eartha* (child girl, 8 years old, 30.17 Kg), selected from the Virtual Family[22] has been used in this study. This model has a resolution of $2 \times 2 \times 2\ mm^3$ and is composed of 75 biological tissues. It should be noted that the choice of a child model is motivated by the computation constraints. In fact, we needed to use a model having a small size to reduce the FDTD simulation time.

Using a deformation tool (EMPIRE Poser [23]), two postures characterizing different wireless device usages, which are respectively a voice configuration with a mobile phone close to the head and a laptop configuration on the knees, have been considered. Numerically, the power absorbed is quantified by the SAR and given by:

$$SAR = \frac{\sigma E^2}{2\rho} \quad (W.kg^{-1}) \qquad (2)$$

Where σ ,ρ and E are respectively the conductivity, the mass density of the tissues, and the local electric field strength in the tissues, which are frequency dependent [24]. In this study, we focus only on the whole body exposure (SAR_{wb}), given by the ratio of the absorbed power to the body's weight.

B. Personal device models

Two personal device models have been designed with a resolution of $2 \times 2 \times 2\ mm^3$: a generic mobile phone and a 3G USB dongle (Fig. 2 and Fig. 3). The antenna geometry has been taken into account during the design to ensure a good return loss performance. The basic components of the

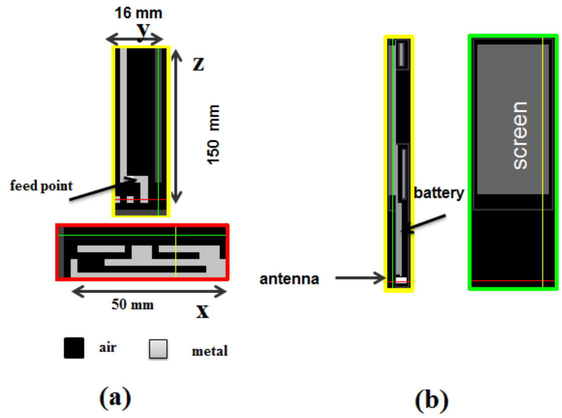

Fig. 2. Mobile phone : (a) geometry of the antenna, (b) antenna location.

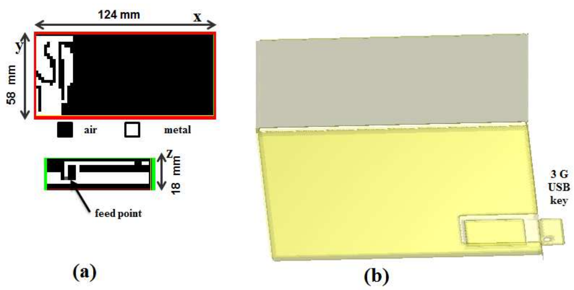

Fig. 3. Laptop :(a) geometry of the antenna 3G USB Key, (b) antenna location.

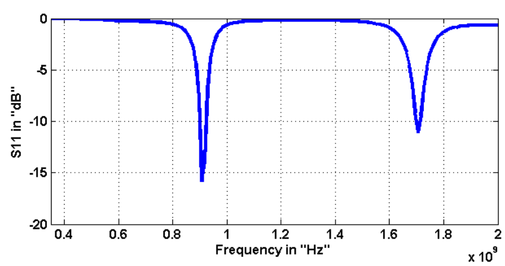

Fig. 4. S_{11} of mobile

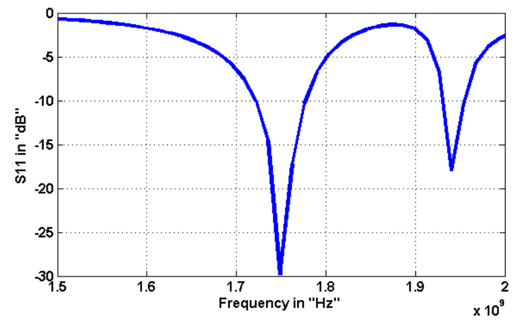

Fig. 5. S_{11} of laptop

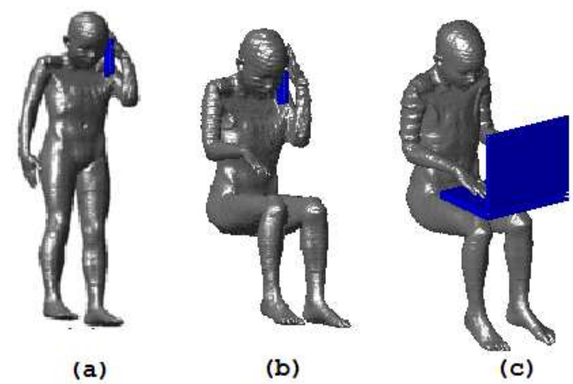

Fig. 6. Postures for Eartha model: (a): standing (voice mode), (b): sitting (voice mode) and (c): sitting with the laptop (data mode; the 3G USB-Key is located close to the left hand)

TABLE I
THE ABSORBED POWER AND THE SAR_{wb} NORMALIZED TO 1 W INPUT POWER.

	radiation efficiency (%)	absorbed power (%)	SAR_{wb} $W.kg^{-1}$
Voice-standing (900MHz)	10	90	0.029
Voice-sitting (900 MHz)	10	90	0.029
Laptop (1940 MHz)	75	25	0.008

devices, such as the battery, patch antenna, and ground plane are arranged in a parallelepipedic box of $52 \times 122 \times 16$ mm^3 for the mobile phone and $134 \times 183 \times 148$ mm^3 for the laptop. Next, the antennas have been simulated with an internally developed FDTD code in a reference environment (free-space). In both simulations, acceptable results have been obtained concerning the impedance and the reflection coefficient of the antenna (see Fig. 4 and Fig.5).

To create realistic configurations, the devices were placed close to the numerical phantom consistently with the usage scenario: near the ear (touch) in the case of a voice posture and on the knees in the case of the laptop (Fig. 6).

C. FDTD simulations

We simulated the 3D gain patterns of both antennas by FDTD. The simulations were performed at 900 MHz for the mobile phone and at 1940 MHz for the laptop. The patterns in azimuth and elevation have been computed with a resolution of 5 degrees.

IV. GAIN PATTERNS AND INPUT POWER STATISTICS

In this part, some results showing the human body effect on the antenna gain are shown. Table 1 presents the percentage of the power absorbed by the body, the overall radiation efficiency and the SAR_{wb} obtained with the various postures. It should be noted that the SAR_{wb} values have been normalized to an input power of $1W$.

We noticed that 90% of the energy is absorbed by the human body with the mobile phone, whereas only 25% is absorbed with the laptop. It should be noted as well that most of the power is absorbed respectively by the head and by the left hand, forearm and thigh in the case of the laptop. In fact, the rate and the amount of absorption are very sensitive to the penetration depth of the electric field, which depends

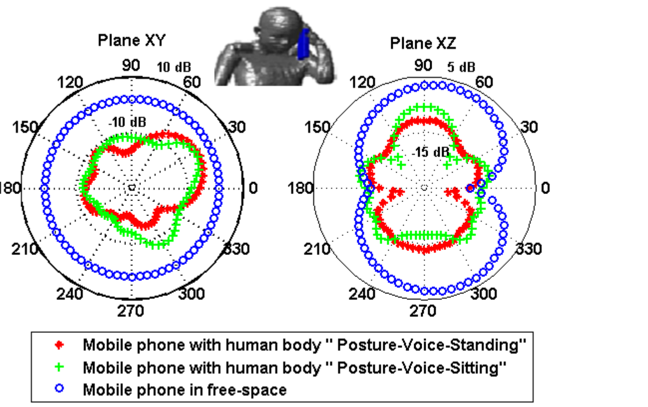

Fig. 7. Comparison of radiation patterns of the mobile phone in free space and in the presence of human body.

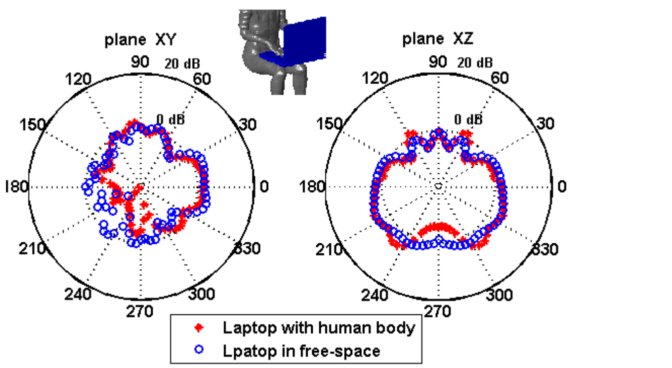

Fig. 8. Comparison of radiation patterns of the laptop in free space and in the presence of human body.

essentially on the frequency and tissue parameters. Also, the distance between the personal device and the human body constitutes a major factor impacting the amount of the losses in the body.

Moreover, the global efficiency of the mobile phone (around 10%) has been significantly affected as compared to the laptop (around 75%).

Fig. 7 and Fig. 8 present the variation of the gain both in free space and in the presence of the human body. The impact of the body on the gain pattern is, as anticipated, very significant in the case of the mobile telephone and more marginal for the laptop.

The gain is reduced to less than $-15dBi$ in certain angular regions (Fig. 7), due to the blocking and the absorption by the body, especially by the head and the hand as was already mentioned. In the *xy* plane, the omnidirectional radiation of the antenna in free space becomes more directional due to the masking and reflection effects of the body. In particular, the human head acts as a reflective surface for the radio waves. In the *xz* plane, a slight increase in gain in certain directions can be noticed due to the reflection by the head.

In the case of the laptop (Fig. 8), the gain variation is smaller than that obtained in the mobile phone case. This can be explained by the farther distance between the 3G USB dongle and the human body. The gain pattern is actually almost identical to the free space pattern, as shown in the two planes. The small difference between both stems from the reflection of waves by Eartha's body. In the *xz* plane, the effect of the left leg is observable around the direction $\theta = 270^0$.

TABLE II
EARTHA-VOICE-STANDING-900MHZ : PARAMETERS OF THE DISTRIBUTIONS.

	IG (μ, λ)		LN (μ, σ)	
	μ	λ	μ	σ
Parameter	18.41	25.95	2.64	0.74
R^2	0.9306		0.9370	

Since the exposure is proportional to the input power delivered to the device, which depends on the many parameters involved, a statistical analysis of this physical quantity is required in the modeling of the exposure. Based on relationship (1), the delivered input power can be written in the following form :

$$P_{in} = \frac{\alpha}{G_e(\Omega_S, \phi_{LOS}, \theta_{LOS})} \quad (3)$$

where α is arbitrarily chosen equal to $1mW$. As mentioned in the section II, the gain $G_e(\Omega_S, \phi_{LOS}, \theta_{LOS})$ depends on the relative orientation ($\Omega_S(\phi_S, \theta_S)$) of the transmitter system with respect to the base station. To simplify computations, ϕ_S and θ_S are assumed to follow a discrete uniform distribution over $[0^o, 360^o]$ and $[-45^o, +45^o]$, respectively. During the post-processing, a considerable interest is granted to the limitation of the maximum power that can be delivered to the mobile phone. Particularly, in the case of GSM-900, the average input power delivered to the mobile antenna is always limited to a threshold power of $250mW$. For that reason, it is crucial to apply a threshold on the empirical power values. The statistical distribution of the DOD translates into a statistically distributed transmitted power, by virtue of equation (3). Several analytical distributions have been tested in comparison to the observed distribution including Log-normal, Weibull, Rayleigh, Exponential, Inverse Gaussian and Gamma distributions. The results revealed a reasonable fit for both Inverse Gaussian and Log-normal distributions denoted respectively by $IG(\mu, \lambda)$ and $LN(\mu, \sigma^2)$. The goodness of fit tests was based on the log-likelihood criterion. Actually, the fit tests showed that the coefficients of determination (R^2) [25] obtained with both distributions were practically the same and very close to 1, which allows us to say that any of these two distributions is acceptable.

The corresponding parameters are given in Tables II, III and IV. The empirical PDF of power values along with the best fits is given in: Fig. 9-11. In these figures, a zoom in the x-axis has been applied in order to display only the power values lying below the 95th percentile.

a. voice posture case

Fig. 9 and Fig. 10 show that the delivered input power depends strongly on the local attenuation caused by the body shadowing effects. It is very clear that it increases logarithmically with the attenuation level. In this respect, the quasi

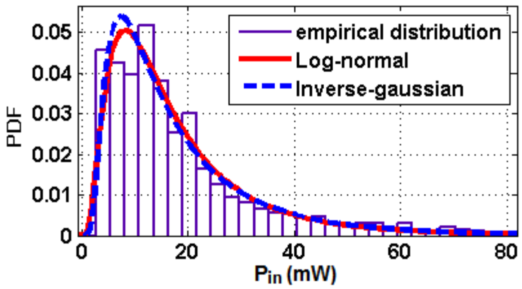

Fig. 9. Comparison between the empirical and the analytical distributions function obtained with the posture "Eartha-voice-standing-900MHz".

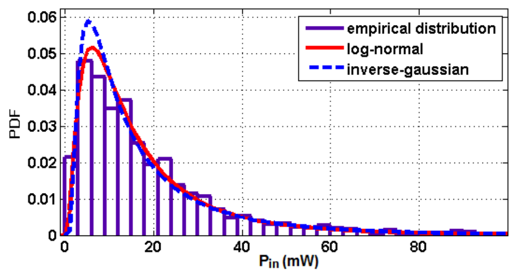

Fig. 10. Comparison between the empirical and the analytical distributions function obtained with the posture "Eartha-voice-sitting-900MHz".

TABLE III
EARTHA-VOICE-SITTING-900MHZ : PARAMETERS OF THE DISTRIBUTIONS.

	I.G (μ, λ)		LN (μ, σ)	
	μ	λ	μ	σ
Parameter	18.60	17.17	2.56	0.87
R^2	0.9301		0.9301	

lognormal character of the distribution is not surprising. This statistical behavior remains typical of Body Area Networks [26].

Between the two voice postures (standing and sitting), a small variation in the parameters of the distributions is noticed. This is due to the fact that the antenna gain is mainly affected by the upper body portion. The latter is not perfectly identical in both postures, in spite of the identical positions of the hand and the hand + head with respect to the mobile phone. This is due to a few constraints in building the computerized body models.

Since the power delivered by the phone amplifier is limited, the choice of α can affect the shape of the distribution. For example in the case of $\alpha = 10mW$, the distribution of the delivered input power is the slice of the distribution obtained with $\alpha = 1mW$ truncated at 25 mW (respectively $2.5mW$ for $\alpha = 100mW$). We have noticed that for α lower than $1mW$ the distribution of the delivered input power is substantially the same, as the parameters are linearly dependent on α.

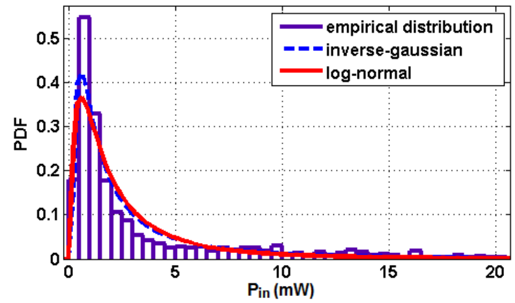

Fig. 11. Comparison between the empirical and the analytical distributions function obtained with the posture "Eartha-Laptop-1940MHz".

TABLE IV
EARTHA-LAPTOP-1940MHZ : PARAMETERS OF THE DISTRIBUTIONS.

	I.G (μ, λ)		LN (μ, σ)	
	μ	λ	μ	σ
Parameter	3.32	1.74	0.58	1.06
R^2	0.9652		0.922	

b. laptop posture case

In the case of laptop, the variability of the delivered input power is not very large. The high peaks of input power are up to $20mW$, which is smaller than those noticed with the mobile phone. These results can be explained by the fact that the 3G USB dongle is placed away from the human body (see Fig. 11).

V. IMPACT OF THE PERSONAL DEVICE POSITION

The induced proximity effects of human body depend on the positioning of personal device with respect to the human body. To highlight this issue and study the variability of the SAR_{wb}, induced by a mobile phone placed in different positions, 40 FDTD simulations were carried out.

The first step consisted in building a set of computer models (body+device) representing a "typical" set of ways to handle the phone by the user. To that aim, the mobile phone was maintained in *cheek* position (EN 62209-1) [27] where the phone was touching the ear and was in weak proximity with the user cheek. Then, the mobile was pivoted against the pinna and moved from the mouth by an angle θ between 0^o and 25^o and vertically by a second angle ϕ varying between -15^o and $+15^o$ (Fig. 12). To ensure a set of samples that more precisely reflected the random positions of mobile phone, 40 experiments were generated by the Latin Hypercube Sampling method (LHS)[28].

At first, we analyze the dependence of the exposure on the mobile phone position, without consideration of the propagation channel and with a fixed delivered power (i.e. no power control). As a result, it is clearly noticed that the proportion of power absorbed by the body varied between 80% and 93%, depending on the phone position. Concerning the exposure level, the mean value of SAR_{wb} (SAR_{wb}^{mean}) is around $0.028\ W.kg^{-1}$ (normalized to a fixed input power of $P_{in}= 1W$) while the coefficient of variation (CV_{SAR}),

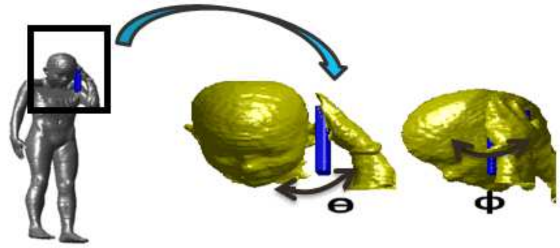

Fig. 12. Definition of position angle.

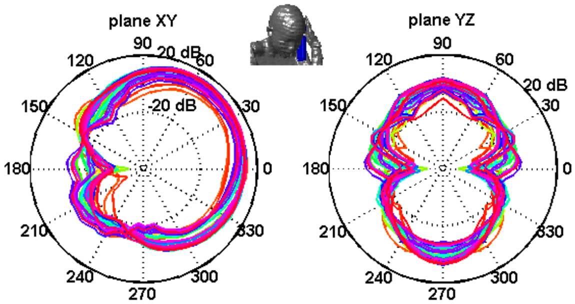

Fig. 13. Impact of body on radiation pattern.

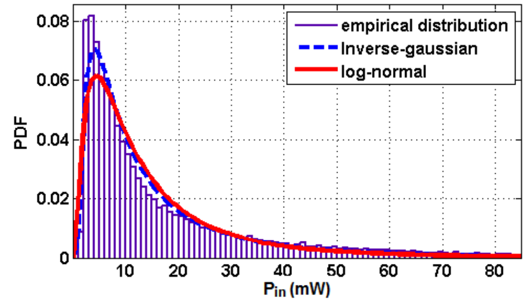

Fig. 14. Comparison between the empirical and the analytical distributions function obtained with the 40 positions.

TABLE V
EARTHA-VOICE-40 TESTED POSITIONS-900MHZ : PARAMETERS OF THE DISTRIBUTIONS.

	I.G (μ, λ)		LN (μ, σ)	
	μ	λ	μ	σ
Parameter	16.64	12.77	2.371	0.94
R^2	0.9632		0.9197	

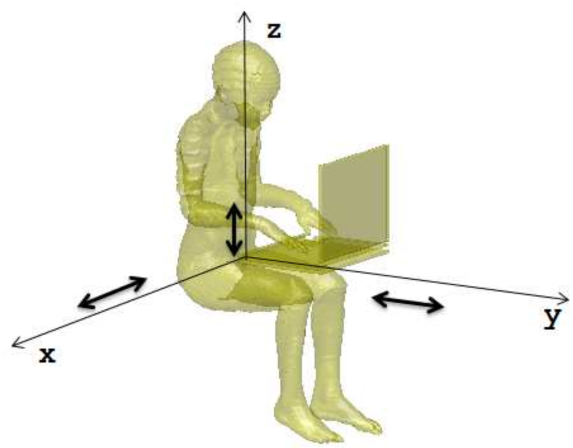

Fig. 15. Definition of laptop position

defined as the ratio of the standard deviation to the mean, is 3%. Although the influence of the device position of the whole body SAR_{wb} is negligible, a significant variation of the exposure in the head "alone" has been observed. In 20% of the number of positions, the absorbed power was 25% higher than that obtained in the cheek position, considered to be the reference position. Moreover, the whole-head SAR (SAR_{head}) variation reached around a mean of $0.16\ W.kg^{-1}$ as characterized by a $CV_{SAR-Head}$ value up to 18%. These results are enlightening with respect to the numerical values described in section IV, since the coefficient of variation of the input power delivered to the mobile phone in a fixed position (CV_{Pin}), i.e., $\sqrt{e^{\sigma^2}-1}$, is higher than 85% as the result of the LOS direction randomness. This simple but important observation expresses that, the exposure is mostly determined by the delivered input power, which depends on the antenna gain and the propagation scenario, rather than by the way the user holds the phone. Given this first conclusion, the effect of human body on the antenna gain is now briefly studied in terms of radiation patterns. For all of testing positions, the radiation patterns obtained with the 40 phone positions showed almost the same behavior, characterized by a severe distortion due to the head and hand proximity. The degradation level is dependent on the position of the personal device with respect to the human body. A variation of up to 10 dB in the antenna gain has been obtained over the 40 simulations (see the thickness of the graph shown in Fig. 13), depending on the radiation direction.

To study the joint impact of the mobile phone position and the propagation channel on the variability of the delivered input power, both types of simulations have been combined during the post processing. The same methodology and propagation scenario (LOS) described in the sections II and IV have been kept. Fig. 14 shows the distribution of the delivered input power compared to analytical distributions, together with best fit analytical distributions.

As can be seen, the statistical tests show that the Inverse Gaussian and the Log-normal remain the most suitable fitting distributions. The R^2 values for these distributions are always higher than 0.9 (see TABLE V). Furthermore, the CV_{Pin} is about $119.\%$. This means that varying the orientation of the transmitter system with respect to the base station can increase by more than two times the delivered input power and consequently the SAR_{wb}.

Turning now to the laptop posture, the influence of the position has been studied by translating the computer in three directions with respect to the knees, as shown in Fig. 15.

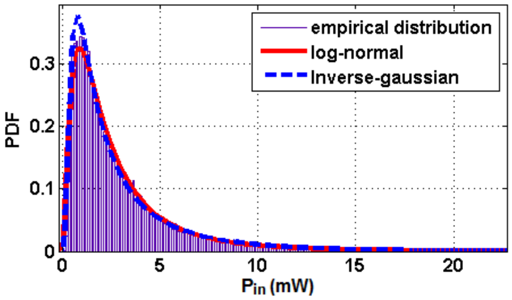

Fig. 16. Comparison between the empirical and the analytical distributions function obtained with the posture "Eartha-Laptop-1940MHz".

TABLE VI
EARTHA-LAPTOP-40 TESTED POSITIONS-1940MHZ : PARAMETERS OF THE DISTRIBUTIONS.

	I.G (μ, λ)		LN (μ, σ)	
	μ	λ	μ	σ
Parameter	3.08	2.64	0.70	0.91
R^2	0.9911		0.9937	

Briefly, the computer undergoes three translations along the three directions $\vec{x}$, $\vec{y}$ and $\vec{z}$ with a Δ_x, Δ_y and Δ_z varying in [-5 cm : 5 cm], [-0 cm : 6 cm], and [-1 cm :1cm], respectively. We have again tested 40 generated samples using the LHS method. Accordingly, the power absorbed has been found to range between 17% and 35%. For a given input power ($P_{in}= 1W$), the maximum SAR_{wb} value is around $0.011\ W.kg^{-1}$. It is obtained when the 3G USB dongle is located very close to the knees. The mean value SAR_{wb}^{mean} is around $0.007W.kg^{-1}$. By excluding the impact of the propagation channel and the variability of the delivered input power in processing the data, the coefficient of variation of whole body exposure (CV_{SAR}) can be up to 18%. As regards the antenna characteristics, some variations in the radiation patterns are observed. However, they remain low compared to those obtained with the mobile phone. Thus, the variability of the delivered input power resulting from the antenna gain variability is reduced compared to that seen with the mobile phone. Regarding the statistical tests of the delivered input power (shown in Fig. 16 and the TABLE VI), we also found that this power could be modeled by an Inverse Gaussian or a Log-normal, with the same goodness of fit.

Overall, the CV_{Pin} is around 113.5%. Consequently, the degree of variability of SAR_{wb} that originates from the fluctuations of the antenna gain overtakes by more than 6 times that stemming from the laptop random position. Obviously, the impact of the device position on the exposure variability is far less than that of the propagation channel. Hence, in the following, we reduce the size of the statistical set by first computing the average exposure SAR_{wb}^{mean} over all device positions for a fixed input power. The remaining variability, is due to the input power delivered to the device in order to mitigate the variable propagation loss.

VI. IMPACT OF MULTIPATH PROPAGATION

In Sections IV and V, we focused on the case of a single dominant path (i.e., LOS) between the transmitter and the receiver. We now address the case of significant multipath components, which often occurs in practice due to reflection, refraction, and diffraction of the radio wave by physical obstacles. These paths often make a significant contribution to the total received power. We compute this power as a simple sum of average powers over all multi path components. This assumption, which neglects any destructive/constructive interference between multipaths, is made because in practice such an interference is highly varying in time and it does not make sense to take it into account in terms of exposure, the mean absorbed power being more relevant than an instantaneous power.

In the present section, we investigate the impact of multipath propagation on the variability of the delivered input power. Based on the reciprocity relationship between a transmitter and the receiver, the input power is rewritten as follows :

$$P_{in} = \frac{\alpha}{\delta_{1,0} a_0^2(\tau_0) G_e(\phi_{LOS}, \theta_{LOS}) + \sum_{k=1}^{k=N} a_k^2(\tau_k) G_e(\phi_k, \theta_k)} \quad (4)$$

Where $\delta_{1,0}$ is a binary variable, taking the value of 1 in the presence of LOS path and 0 otherwise. N, $a_k(\tau_k)$, τ_k and (ϕ_k, θ_k) are respectively the number of paths, the path gain amplitude, the arrival time (at the base station) and the DoD associated with each k-path. The power α is always chosen equal to $1mW$.

In order to evaluate the impact of the propagation channel on the exposure, we here make use of a simplified channel model inspired from the WINNER project channel [29]. This model distinguishes betwseen a set of radio environments, among which we restrict to four of them (denoted by **Env1-4**, with the corresponding WINNER environment classification between brackets):

- **Env1: Indoor " in office" (A2, B4, C4); NLOS**
- **Env2: Urban "in street" (B1,C1); LOS+NLOS**
- **Env3: Bad Urban (B1,C1); NLOS**
- **Env4: Highway "in car" (D1); LOS+NLOS**

The WINNER project provides very detailed propagation models, in terms of spatial and temporal resolution, which is well reflected in concepts like "clusters", main paths and sub-path within these "clusters". For what concerns the exposure assessment, such a refinement is excessive. We adopt the simplification method proposed in (Sibille *et al* 2012) [30], where the number of paths N is assumed to follow a Gaussian distribution, low bounded by 1, with a mean μ_N and a standard deviation σ_N.

Each of these paths is given by departure angles (azimuth ϕ_k and elevation θ_k), which are assumed to be uniformly distributed over $[0^o, 360^o]$ and in $[-40^o, +40^o]$, respectively.

TABLE VII
THE PROPAGATION ENVIRONMENT PARAMETERS.

Scenario	Indoor "in office"	Urban "in street"	Urban "bad"	Highway "in car"
$\boldsymbol{scenario}$	NLOS	LOS/NLOS	NLOS	LOS/NLOS
$\boldsymbol{K(dB)}$				
μ_K/σ_K		9/7		7/6
$\boldsymbol{N}$				
μ_N/σ_N	10.6/2.4	6/3.5	14/3	7/6
$\boldsymbol{a_k}$				
$\sigma_\tau(ns)$	25	55	55	25

According to the results of the measurement campaigns of the WINNER project, the power delay profile [31] is an exponential decay function. Consistently with this tendency, we can define the path gain amplitude as:

$$a_k^2(\tau_k) \propto e^{-\frac{\tau_k}{\sigma_\tau}} \tag{5}$$

where the arrival times τ_k are uniformly distributed and σ_τ is the empirical root mean square (rms) delay spread, known as the standard deviation of the paths delays [32].

Depending on the availability of LOS path, the Rician K factor can be written as :

$$K = \frac{a_0^2(\tau_0)}{\sum_{k=1}^{k=N} a_k^2(\tau_k)} \tag{6}$$

where the LOS component is considered to be deterministic and the rest of the multipath to be random. In the expression above, a normalization is enforced, through the sum all of the squares of these coefficients (including $a_0(\tau_0)$) equal to 1.

$$\sum_{k=0}^{k=N} a_k^2(\tau_k) = 1 \tag{7}$$

Furthermore, the K factor is assumed to follow a Log-normal distribution, given by its mean μ_K and its standard deviation σ_K. Given the type of statistical distributions considered above, it is straightforward to generate realizations of the set of multipaths respecting these distributions. The parameters used for the simulations below (in for the four environments) are displayed in Table VII.

The multipath scenario is simulated using the same numerical models used in the section IV. Both configurations, voice at 900 MHz and Laptop at 1940 MHz, while maintaining a fixed position of the personal device, are used. In order to investigate sufficiently accurately the statistical features of the delivered input power, a large number of multipath propagation experiments have been generated ($\mathbf{10000}$ for each value of N).

Again, the input power was found to show a logarithmic behavior. Similarly to the results observed with LOS scenario, the Log-normal and the Inverse gaussian remained the most suitable distributions to characterize the variability of the delivered input power.

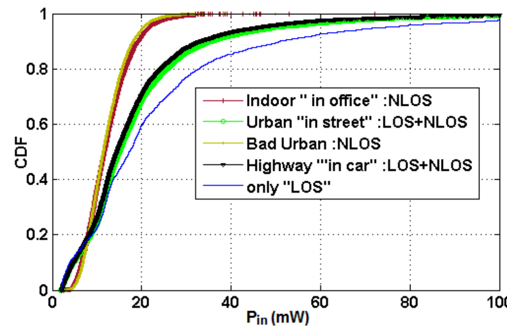

Fig. 17. Comparison between the CDF obtained with the posture "Eartha-voice-standing-900MHz".

In Fig.17 and Fig.18, we show the cumulative distribution functions (CDF) of the delivered input power for various propagation environments, respectively for the laptop use and the mobile phone use. Examining these curves, we can notice that variability indicators of the delivered input power, such as the mean and the coefficient of variation CV_{Pin}, depend on the type of propagation environment. Three main classes of propagation environment can be distinguished: NLOS propagation (**Env1, Env 3**), combined LOS/NLOS propagation scenario (**Env2, Env 4**) and a typical LOS propagation scenario (**section II-III**).

In the NLOS case, i.e., by excluding the LOS path, the distribution of the delivered input power becomes narrower with a CV_{Pin} around 41%, representing one-third of that obtained in the LOS scenario (i.e., single path communication). As a matter of fact, the multipath scenario reduces the effect of the gain variability. Adding additional paths results in an averaging of the delivered input power, which reduces the impact of the directional heterogeneity in the gain. This multipath diversity effect decreases as well the appearance of large peaks values of the power, which were encountered in the case of LOS. In the case of combined LOS/NLOS propagation, the mentioned averaging still exists, but its impact on the non-uniformity of the antenna gain is smaller than the previous case (NLOS scenario). This can be explained by the impact of the Rician K factor generated, limiting the contribution of the other paths in the input power. The larger K, the more the LOS component dominates. In such case, i.e., in a typical LOS scenario, the input power is directly related to the local partial gain, and the chance to fall either into a pattern dip or into a pattern maximum is significant.

For a more comprehensive understanding, the mitigation effect of the propagation environment has been studied as a function of the number of paths. For the sake of space limitation, only the mobile phone case is presented here, within two propagation scenarios: NLOS scenario (**Env 1**) and combined LOS/ NLOS scenario (**Env2**).

Fig. 19 and Fig. 20 present, respectively, the coefficient of variation and the mean of the delivered input power versus the number of path N.

In the **Env1**, there is indeed a rapid decrease in the CV_{Pin} when increasing the number of paths from 1 to $\mathbf{20}$. Varying the number of paths between $\mathbf{20}$ and $\mathbf{100}$ makes the CV_{Pin}

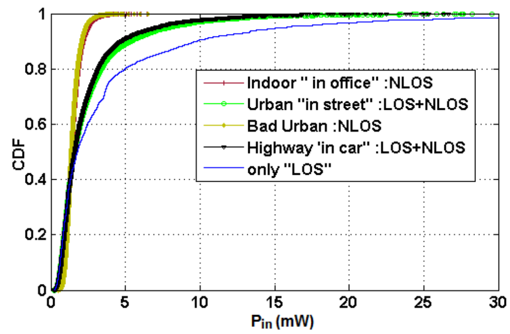

Fig. 18. Comparison between the CDF obtained with the posture ”Eartha-Laptop-1940MHz”.

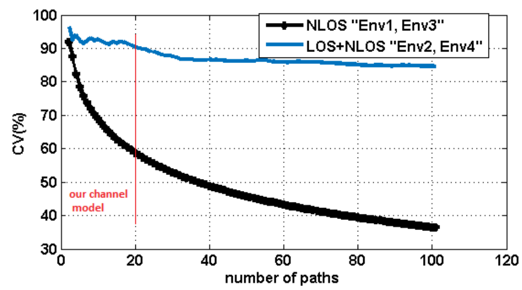

Fig. 19. CV_{Pin} vs. number of paths

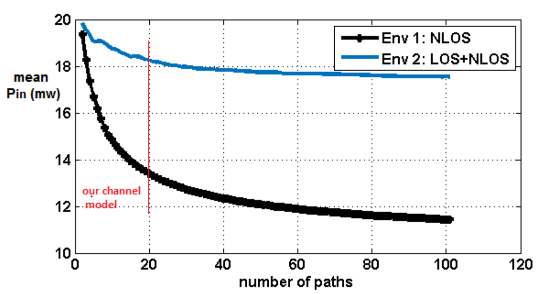

Fig. 20. Average input power vs. number of paths.

varies from 60% to 30%. On the other hand, the mean input power decays roughly exponentially (see Fig. 20) down to 12 mW for 20 paths, representing a reduction of more than 30% with respect to the LOS scenario, 18 mW.

In **Env2**, CV_{Pin} and the mean input power show a slight decrease, as compared to the LOS case. This comes from the fact that the contribution of NLOS paths is bounded by the Rician K factor.

The above analysis has been carried out with a fixed position of the personal device. Our main finding is that the contribution of the propagation environment, especially in pure NLOS environments, is essential as regards the variability of the input power as well as of the associated exposure: multipath diversity significantly reduces the exposure variability. From a statistical point of view, the propagation related exposure variability no longer dominates over the device positioning related variability.

This last part is devoted to determining the CDFs of the SAR_{WB} from the proportional existing between the induced exposure and the input power delivered to each device. Fig.21 and Fig.22 show, respectively, the CDFs of SAR_{WB} induced by the mobile phone (900 MHz) and of that induced by the computer (1940 MHz). We note that SAR_{WB} values are far below recommended limits ($0.08W/kg$).

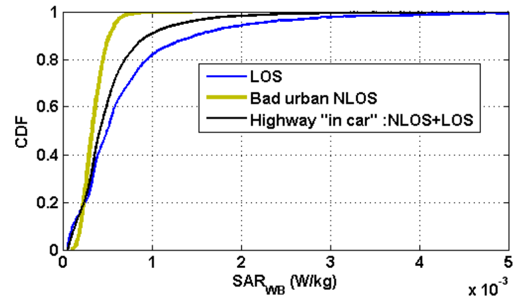

Fig. 21. Comparison between the CDFs of the SAR_{WB} obtained with the posture ”Eartha-voice-standing-900MHz”.

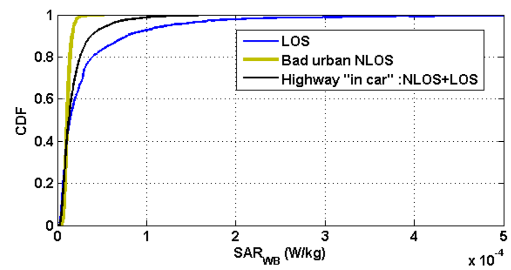

Fig. 22. Comparison between the CDFs of the SAR_{WB} obtained with the posture ”Eartha-Laptop-1940MHz”.

VII. Summary and Conclusion

In this work, a methodology dedicated to characterize the variability of the input power delivered to wireless personal devices under specific propagation assumptions is introduced, based on a refined device description and full body electromagnetic simulations.

For this purpose, a series of cases and device+body configurations have been simulated and analyzed in order to study the influence of the type of personal device and of its positioning with respect of the human body, as well as the effect of the operating frequency on the variation of exposure level and on the degradation of the antenna's radiation pattern. The results, well supported by the existing literature, show that the performance of the antenna is affected significantly in terms of radiation efficiency as well as shape of the radiation patterns, especially in the case of a mobile phone use for voice calls. This observation is reflected in the absorption of a large portion of radiated power by the head and the hand and also in the partial reflection of the waves by the body. Furthermore, the degradation of the radiation efficiency and the exposure dose showed a (moderate) sensitivity to the position of the personal device with respect to the human body, particularly in the case of the laptop.

In a wireless network context, the exposure has been found to be strongly dependent on the local propagation environment, owing to the power control enforced by most wireless communications standards. This was addressed by combining the SAR$_{wb}$ value (calculated for a constant power) with a statistical distribution of the delivered input power, for various user positions. Accordingly, two correlated distributions of the delivered input power need be characterized: that expressing the dependence on the position of the device with respect to the body and that expressing the impact of the propagation channel (e.g., the number of paths, their attenuation and the departure angles).

This study focused in a large part on the modeling of the delivered input power under different propagation scenarios, mainly distinguishing between LOS and NLOS (or combined LOS/NLOS) scenarios. In the NLOS scenarios, we are particularly interested to investigate random indoor/outdoor configurations while stressing the contribution of the diffuse multipath components, often characterized by higher randomness, on the total input power.

The results showed that the influence of the body on the variability of the delivered input power is fairly weak, especially in the LOS scenario where the impact of propagation on the variability dominates. In both scenarios, the statistical analysis proves that the Log-normal distribution provides quite a satisfactory fit to the empirical values, referring also to its simplicity in terms of implementation and usage.

Due to the computational cost of FDTD simulations, a limited number of models (human body and wireless devices) have been used in this work. Since these models do not reflect sufficiently the variability of use cases and user characteristics, the obtained results are a first step towards the assessment of exposure to electromagnetic fields in the context of wireless networks. Further work is planned in the future for a more complete coverage.

Nevertheless, the results obtained and the strategies examined in this study make a practical guidance to use in the characterization of real exposure, when using other user models, other personal devices working in others frequencies.

References

[1] ”ICNIRP guidelines for limiting exposure to time varying electric, magnetic, and electromagnetic field (up to 300 GHz)”, *Health Phys, vol 74,* pp. 494 522, 1998.

[2] M.A.Stuchly, M.Rahman, M.Potter, T.Williams , ”Modeling Antenna Close to the Human Body”, *Aerospace Conference Proceedings, 2000 IEEE, vol. 5* pp. 83 - 89, 2000.

[3] H.R Chuang, ”Human operator coupling effects on radiation characteristics of a portable communication dipole antenna ”, *IEEE Transactions Antennas and Propagation, vol. 42* pp. 556-560, 1994.

[4] Yu-Huei Tseng, Wen-Shyang Hwang, Ce-Kuen Shieh, ”The Influence of Propagation Environment in a Live GSM Network”, *Journal of electrical engineering,* pp. 1 - 7, 2009 2012.

[5] A. Sibille, ”Statistical Modeling of the Radio-Electric Properties of Wireless Terminals in their Environment”, *IEEE Antennas and Propagation Magazine,* pp. 117 - 129, 20 december 2012.

[6] J.Wiart, A.Hadjem, N.Varsier, Nadge E.Conil, ”Numerical dosimetry dedicated to children RF exposure” , *IProgress in Biophysics and Molecular Biology,* pp. 421-427, December 2011.

[7] Wang, Z., Univ. of London, UK, Chen, X., Parini, C.G., ”Effects of the ground and the human body on the performance of a handset antenna”, *IEEE Antennas and Propagation Magazine,* pp. 131 - 134, Apr 2004.

[8] T. Tuovinen, M. Berg, K. Yekeh Yazdandoost, E. Salonen, and J. Iinatti, ”Radiation properties of the planar UWB dipole antenna in the proximity of dispersive body models”, *BodyNets '12 Proceedings of the 7th International Conference on Body Area Networks,* pp. 82- 88, 2012

[9] J. Ryckaert, P. De Doncker, R. Meys, A. de Le Hoye and S. Donnay, ”Channel model for wireless communication around human body”, *Electronics Letters, vol.40, no.9,* pp. 543-544, April 2004,.

[10] K. Ogawa, T. Matsuyoshi, and K. Monma, ”An analysis of the performance of a handset diversity antenna influenced by head, hand, and shoulder effects at 900MHz. Part I. Effective gain characteristics” , *IEEE Transactions on Vehicular Technology, vol. 50, no. 3* pp. 830844, 2001.

[11] C. H. Li, E. Ofli, N. Chavannes, and N. Kuster,” Effects of hand phantom on mobile phone antenna performance”, *IEEE Transactions on Antennas and Propagation, vol. 57, no. 9*, pp. 27632770, 2009.

[12] Jensen and Rahmat-Samii Y,” The electromagnetic interaction of handset antennas and a human in personal communications. ”, *Proc. IEEE vol. 38*, pp. 717, 1995.

[13] K.H.Ng, E.K.Tameh and A.R.Nix, ”A New Heuristic Geometrical Approach for Finding Non-coplanar Multiple Edge Diffraction Ray Paths”, *IEEE Transactions on Antennas and Propagation, Vol. 54, No. 9* pp. 2669-2672, September 2006.

[14] J. Toftgard, S.N. Hornsleth, J.B. Andersen, ”Effects on Portable Antennas of the Presence of a Person ” , *IEEE Transactions on Antennas and Propagation, vol. 41, no. 3* pp. 739746, June 1993.

[15] A. Taflove and M. Brodwin , ”Numerical Solution of Steady-State Electromagnetic Scattering Problems Using the Time-Dependant Maxwells Equations” , *European Microwave Conference Proceedings, 3* , pp. 4-6, 2005.

[16] W. Jakes, ”Microwave Mobile Communications” , *New York: Wiley* , 1974.

[17] EU FP7 LEXNET (low EMF exposure future networks) project. [Online]. Available: http://www.lexnet-project.eu/

[18] A. Balanis, Antenna Theory, 2003, John Wiley and Sons Inc.

[19] Thomas M. Cover, Joy A. Thomas, ”Elements of Information Theory ”, New York: Wiley, 1991. ISBN 0-471-06259-6

[20] C. Berrou, A. Glavieux, and P. Thitimajshima, ”Near Shannon limit error-correcting coding and decoding: Turbo codes” , *in IEEE Int. Conf. Communications (ICC)*, pp. 1064-1070, 1993.

[21] Shittu, W.A., Bajoga, B.G. Anwar, F. Salami, M.J.E, ”Prediction of received signal power and propagation path loss in open/rural environments using modified Free-Space loss and Hata models ” , *RF and Microwave Conference, 2008. RFM 2008. IEEE International,* Kuala Lumpur, pp. 126 - 130, 2-4 Dec 2008

[22] A.Christ, W.Kainz, E.G. Hahn , K. Honegger, M. Zefferer , E. Neufeld E, W. Rascher , R. Janka , W. Bautz, J. Chen , B. Kiefer, P. Schmitt , H.P. Hollenbach, J. Shen , M. Oberle , D. Szczerba , A. Kam, J.W Guag, N. Kuster, ”The Virtual Family–development of surface-based anatomical models of two adults and two children for dosimetric simulations” *Physics in Medicine and Biology, vol. 55, no. 2*, pp. 2338, January 2010.

[23] EMPIRE-XCcel , *http://www.empire.de/page11.html*

[24] C. Gabriel, ”Compilation of the dielectric properties of body tissues at RF and microwave frequencies”, *Brooks Air Force Base, Brooks AFB, TX, Tech. Rep. AL/OE-TR-1996-0037*, 1996 [Online]. Available: http://transition.fcc.gov/oet/rfsafety/dielectric.html

[25] Steel, R.G.D. and J.H. Torrie, 1960, ”Principles and Procedures of Statistics with Special Reference to the Biological Sciences, *New York, McGraw-Hill Book Co. Inc.*, 481 p., 16-20 May 2005.

[26] A. Fort, C. Desset, J. Ryckaert, P. De Doncker, L. Van Biessen, and S. Donnay, ”Ultra Wide-band Body Area Channel Model, *IEEE International Conference on Communications”, vol. 4 no. 9*, pp. 2840-2844, 16-20 May 2005.

[27] EN 62209-1 ”Human exposure to radio frequency fields from hand-held and body-mounted wireless communication devices Human models, instrumentation, and procedures Part 1: Procedure to determine the specific absorption rate (SAR) for hand-held devices used in close proximity to the ear (frequency range of 300 MHz to 3 GHz)”.

[28] M. D. McKay, R. J. Beckman, and W. J. Conover, ”A comparison of three methods for selecting values of input variables in the analysis of output from a computer codel”, *Technometrics , vol. 21,* pp. 339-245, 1979.

[29] M. D. McKay, R. J. Beckman, and W. J. Conover, ”IST-4-027756 WINNER II D1.1.1 WINNER II Interim”, *Channel Models v1.0,* December 2006.

[30] A.Sibille, ”Statistical Modeling of the Radio-Electric Properties of Wireless Terminals in their Environment”, *Antennas and Propagation Magazine, IEEE vol. 54,* pp. 117 - 129, December 2012

KRAYNI ANIS was born in Tunisie on February 13, 1987. He received her engineering degree in Telecommunications from The High School of Communications in Tunis (Sup'Com), Tunisia in 2011, the M.Sc. degree in Computer Science from the University Paris-Est Marne-la-Valle sity (Paris VI), Paris, France, in 2012, and is currently working toward a Phd at Orange Labs, Issy Moulineaux, France. His research interests include the study of electromagnetic radiation exposure and the modeling of user-shadowing effects in wireless channels.

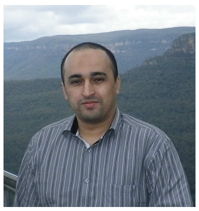

Abdelhamid Hadjem received the Eng degrees in electrical engineering from the Science and Technology University. Algiers, Algeria, in 1999, the M;Sc. degrees in electronics from the Pierre and Marie Curie University (Paris VI), Paris, France, in 2001, and Ph.D. degree in electrical engineering from Paris VI university and research and development of Orange Labs., Paris, France, in 2005. Since 2006, he has been with Orange (former the research and development, France Telecom), Issy les Moulineaux, France. His research interests are electromagnetics for telecommunications systems and biomedical application of numerical electromagnetic techniques.

Alain Sibille graduated from Ecole Polytechnique (1977) and from Telecom-ParisTech (1979) in France and obtained the PhD/habilitation degree from University of Paris 7 in 1985. He first conducted basic research within France-Telecom R&D and later as a part time independent consultant, then moved to ENSTA-ParisTech where he led the Electronics and Computer Engineering department until 2010. He is currently professor and Vice-Chair for Research of the Communications & Electronics Department at Telecom-ParisTech. His scientific interests lie in ultra wide band communications and systems, and in the interactions between antennas, channels, and signal processing. Prof. Alain Sibille chaired the European Wireless Conference 2007 in Paris and co-chaired the TPC of IEEE-PIMRC 2008. He is a National delegate and coordinator of topical working groups within the ongoing European Cooperation Action COST IC1004 Cooperative Radio Communications for Green Smart Environments. He is also involved in URSI-France as Secretary General.

Christophe Roblin (Member, IEEE) received the degree in electrical engineering from the Ecole Nationale Superieure de l'Aeronautique et de l'Espace, Toulouse, France, in 1987 and received the Ph.D. degree in submillimeter receivers for radio astronomy in 1992. Currently, he is Head of the Adaptive Antennas and High Data Rate Radiocommunications Group and Associate Professor at ENSTA-ParisTech (Ecole Nationale Superieure de Techniques Avancees ParisTech), Paris, France. He has a strong experience in microwave circuit and antenna design and modeling. Since 2002, his research activities have been in the area of ultrawideband communications, focussing on UWB antenna design, characterization and parametric modeling. He is also currently involved in antenna and channel topics for body area networks. He has significantly contributed to several European projectsVADAMO (FP4), ULTRAWAVES (FP5), and PULSERS I & IIVand has been the ENSTA team leader for PULSERS I and the French National Research Agency (ANR) project BANET. He has authored or coauthored more than 70 publications and communications.

Joe WIART (SM'02) received the Engineer degree from the cole Nationale Suprieure des Telecommunication, Paris France, in 1992, and the Ph.D. degree in physics from the cole Nationale Suprieure des Tlcommunications (ENST) and Pierre and Marie Curie University (Paris IV), Paris, France in 1995. In 1992, he joined the Centre National d'Etudes des Tlcommunications (CNET) (now Orange) Issy Moulineaux, France, and spent three years involved with propagation in microcellular environments. Since 1994, he has been involved with the interaction of radio waves with the human body and on medical electronic devices. He is currently the head of a group that deals with these questions. His research interests include electromagnetic compatibility (EMC), bioelectromagnetics, antenna measurements, computational electromagnetics, and signal processing. Dr. Wiart is vice chairman of the COST 244 bis, chairman of the CENELEC TC 211 working group in charge of mobile and base-station standards, and vice chairman of the URSI French commission K.